Int. J. Nonlinear Anal. Appl. In Press, 1–9
ISSN: 2008-6822 (electronic)
http://dx.doi.org/10.22075/ijnaa.2023.30223.4369

Application of machine learning to predict daylight glare probability

Seyedeh Tabasom Beykai, Fatemeh Mozaffari Ghadikolaei*, Abdollah Ebrahimi

Department of Architecture, Sari Branch, Islamic Azad University, Sari, Iran

(Communicated by Seyed Hossein Siadati)

Abstract

Daylight Glare Probability (DGP), founded on the latest glare metric, is the main challenge related to daylight glare inside buildings. Studies showed that the DGP depends on several factors, such as vertical illuminance values at the human eye factor, which is an essential parameter. In this study, we implement machine learning techniques to estimate and predict the DGP classifications, which are imperceptible, perceptible, disturbing, and intolerable based on the various influenced factors. A series of machine learning simulations have been conducted to investigate how those factors can be influenced by the degree of glare and classifications. In this research, different machine learning algorithms such as Artificial Neural Networks (multi-layer perceptron), K-Nearest Neighbors (KNN), Support Vector Machines (SVM), and Random Forest (RF) were employed to determine or predict the DGP classifications accurately. Results showed that the RF is the most effective method to classify the DGP and can predict with up to 99% accuracy. Furthermore, the results displayed that vertical illuminance at eye level (lux), Ev, compared with other factors, has the largest influence on the DGP classifications. Consequently, machine learning is a powerful, promising, and viable option to implement in building constructions to optimize energy consumption, a global issue in the current century.

Keywords: daylight glare probability (dgp), vertical illuminance at eye level (lux), ev, machine learning, artificial neural network; building constructions
2020 MSC: 68T07

1 Introduction

Glare is one of the essential variables in achieving visual comfort and visual quality. However, the glare depends on the direction and position of a space's vision, making it complex to evaluate verified to conventional illuminance-based metrics. Moreover, dealing with glare is still a challenging issue in building design. Today, assessing the discomfort of glare due to glare is still a topic of research and discussion. Many researchers have worked in this field and developed various methods to evaluate glare [3, 10, 21, 28, 31]. Daylight Glare Probability (DGP), in comparison with other available metrics, is one of the most acceptable conducting and robust models to predict glare [16, 19, 31, 32].

Field measurement and software modeling are the main methods used to evaluate indoor daylight performance. In this regard, to better understand glare criteria, Quek et al. [11], under controlled laboratory conditions, evaluated the glare of discomfort in low illuminance conditions with low levels of design compatibility. The results showed that

*Corresponding author
Email addresses: t.beykaeii@gmail.com (Seyedeh Tabasom Beykai), mozaffarifatemeh2@gmail.com (Fatemeh Mozaffari Ghadikolaei), eb1526300@gmail.com (Abdollah Ebrahimi)

Received: January 2023 *Accepted:* April 2023

between the two effects of light radiation, discomfort (Saturation and Contrast), the contrast measures provide glare responses more reliably than combined criteria such as DGP at low compatibility levels [4, 7, 14, 35].

Despite this, DGP may not predict glare well in some scenarios that differ significantly from the development scenarios of DGP. In other words, the relative weight between contrast and saturation may not fit well in extrapolation [37]. Such a condition has attracted the concentration of investigators to the need to modify the criteria for the DGP index. However, other studies on the DGP index show that the index works well in many scenarios due to the effect of saturation and contrast [34, 36]. And may assess glare from frequent reflections of bright sources and direct sunlight falling on the work surface as a cause of glare [18].

In recent years, the use of software such as Radiance, DIVA, Honeybee, and Ladybug is one of the most widely used and popular methods in the analysis of glare based on the probability of daylight (DGP) to improve the quality of life of building residents [13, 27, 29, 33, 38]. So that the use of appropriate solutions in daylight design (that provide visual comfort to improve energy efficiency) can be achieved by considering dynamic simulations and evaluating the results of daylight performance [12]. Established on the examination of the received outcomes, the following can be achieved [15]:

1. Regional application of the main body of the current body on stunning issues as well as emergency proposals; and
2. Provide new experimental data to help the field and, among other things, improve the tools used by day-today professionals.

The simulation study's main issues are the quality of the input data and the interpretation of the output results. A maximum variation of 20% between simulation and measurement appears acceptable, according to a survey by Ochoa et al. [24]. Using different validation and optimization methods helps to confirm the accuracy of the results. As in a study [1], Radiance simulator results showed that all simulated DGPs agreed well with the laboratory tests [1]. In another study, parametric processes and [22] MOO were performed due to a reduction in decision time. Classification Photometric classifications and measurements were collected and analyzed [6].

A Bidirectional Scattering Distribution Function (BSDF) was utilized to compare the measurement and simulation for vertical illumination, near-camera transmission, and the daylight glare probability [2].

In recent investigations, machine learning techniques have been employed to estimate the DGP at the user's level through the appropriate location, number, and type of camera according to its sensors [9, 30]. In order to anticipate the observer DGP, Mentens et al. [23] took the influence of the sun's direction into consideration. Then, a black-box model is constructed utilizing the optimal parameters using artificial intelligence (AI). The findings demonstrate that the ceiling camera and the sun's location may be used to anticipate the DGP from the observer's POV precisely.

Artificial intelligence permits the replication of intelligent behaviors prevalent in complex and constantly changing contexts through its self-adaptive processes [5, 8, 17, 20, 25, 26]. The term "AI" often refers to a computer algorithm's capacity to learn a complex task using intelligently observed perceptions or attributes included in previously used (and potentially repeated) DGP data. The capacity of AI techniques to work independently without relying on intricate mathematical formulas or precise connections between input and output is its distinguishing characteristic. Numerous AIbased Machine Learning (ML) techniques, including Support Vector Machines (SVM) [7, 11, 14], artificial neural networks (ANN) [4, 35, 36, 37], K-Nearest Neighbors (KNN) [18, 34], Random Forests [38], etc., have been proposed and specified in the published literature. In this study, we employ machine learning techniques to predict the DGP. Multi-layer perceptron (MLP) as an artificial neural network, SVM, KNN, and RF have been employed as the primary forecasting methods to predict the DGP classifications. In this study, we showed the application of ML techniques in building design to reduce energy consumption and mitigate CO_2 emissions in the atmosphere. The following sections explain how we can gather the DGP data and the influenced factors. Then we show machine learning results, evaluate the key parameters that impact the DGP classifications prediction estimation, and discuss our findings.

2 Methodology

This paper aimed to realize which parameter has a small influence on the DGP and which parameter has a strong impact. Furthermore, which method of machine learning can predict accurately. For this purpose, we required a dataset for training the DGP classifications.

2.1 DGP dataset

The close relationship between the outside environment and the sense of homeliness inside the building reinforces phenomena related to human existence. Natural light can achieve this by producing a sense of fulfillment and visual comfort. The architectural quality of natural light design must consider visual comfort, glare reduction, and adequate contrast patterns because vision is one of the most vital human senses [28, 31].

Human physical and mental health insurance was the primary driver behind creating and enhancing the interior's spatial and environmental quality. The study and application of daylight are intimately connected to the elements that comprise a crucial step in the design process.

Controlling the sensation of glare is one of the most important aspects that should be considered when facing the problem of visual comfort, especially when irradiated with natural light, so that glare is associated with residents' satisfaction with the indoor space [27]. However, according to age, gender, and previous experience in visual function and perception, residents, have different responses and preferences to daylight [33]. People's perceptions from season to season are different, and in winter, more than the presence of sunlight. Glare might be caused by: a) excessive sunlight in the residents' field of vision; b) the presence of objects whose luminosity is significantly higher than the average background luminosity [29]. c) the reflection of sunlight from other surfaces [13] leads to visual stimulation or eye fatigue. Therefore, inadequate visual contrast, direct sunlight, and annoying glare are the three leading causes of visual discomfort.

In the present study, daylight glare probability (DGP) has been utilized to evaluate glare. The glare is usually the ratio of light sources' size, location, and luminosity which expresses based on the four factors that are as follows [12, 15, 24]:

The luminance of the glare source (Ls): is the average luminance of all source pixels. Luminosity levels can be obtained through photometric simulation in SPEOS software. The luminance of each pixel is acquired with the "GetValueRectangle ()" function. The average luminosity of a glare source can be computed by traversing all the pixels of the light source.

Vertical illuminance (Lv): can be defined as the measure of light perception by the camera and our eyes when reflected off a surface.

The source position index, P, is in contrast to the relative sensitivity to the discomfort glare source at several positions across the field of view which can be estimated by Equation (2.1):

$$P = \exp[(35.2 - 0.31889\alpha - 1.22e^{-2\alpha/9}) \times 10^{-3}\beta + (21 + 0.26667\alpha - 0.002936\alpha^2) \times 10^{-5}\beta^2] \tag{2.1}$$

where α is the angle between the line of sight and the vertical of the plane including the source, in degrees, (here, $\tan^{(-1)}(x/y)$ [deg], y and x are the vertical and horizontal distances [m] between the point of view and the source, respectively). The parameter β is the angle between the line of sight and the line overlooking the source.

Solid angle (ω): is the measurement of that part of space around a point bounded by a conical surface whose vertex is located at that point and is introduced as the ratio of the intersected area of the sphere at the center of that point to the square of the radius of the sphere that is represented as radian [34]. The solid angle is obtained by the below relation:

$$\omega = A \ \cos\theta / I^2 \tag{2.2}$$

where A is source zone, I is the distance between eyes and source, and θ is the angle from the source to the perpendicular plane on which a source is located.

2.2 Machine learning algorithms

Machine learning algorithms are generally data-driven techniques based on multi-disciplinary concepts that merge the statistical inference and power of the computer science which includes optimizations and probability.

Figure 1 illustrates the schematic flowchart of the simple learning pattern involving the different phases which are typically comprehended as:

1. Pre-processing
2. Learning
3. Performance and evaluations

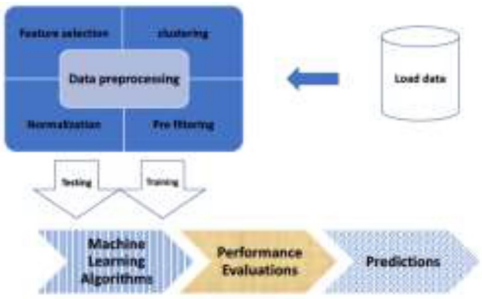

Figure 1: diagram of a machine learning format [1].

An algorithm for an intelligent learning model is began with a delivered collection of labelled data examples that prepare the model's input attributes.

According to Figure 1, the pre-processing step of the learning algorithm is the initial phase and entails data processing methods such feature selection, data normalisation, clustering of the data patterns, etc. Prefiltering is a preliminary method for grouping data with several components. The normalisation eliminates the improper and perhaps unsettling impacts of various input feature variation ranges during the model's training phase. The input-target matrix values are the normalised data values in the 0–1 range. Then duplicate data is added to the input matrix, which is the major focus of the training phase. The machine learning algorithms implemented in this manuscript are listed as follows:

Artificial neural networks (ANN) are biologically motivated computational networks. The ANNs most generally employed for different problems is based on a supervised approach and include three layers: input, hidden, and output.

Support Vector Machines (SVM) are supervised machine learning algorithms for the category and regression computation. The SVM carry out both linear and nonlinear classifications. The nonlinear classification is executed using the Kernel function. In nonlinear classification, the kernels are homogenous polynomial, complex polynomial, Gaussian radial basis function, and hyperbolic tangent function. Some writers have discussed that the usefulness of the SVM approach is more helpful in classification accuracy and the most suitable research performance than other algorithms.

K-Nearest Neighbors (KNN) algorithm is a straightforward, easy-to-implement supervised machine learning algorithm that can crack classification and regression issues [34].

Random Forest (RF), as its name suggests, is made up of numerous unique decision trees that function as a costume. Each tree in the random forest emits a class forecast, and the prediction from our model changes depending on which class receives the most votes.

In fact, it utilizes bagging and randomization in constructing each tree to make an uncorrelated forest of trees whose board forecast is more precise than any one tree. The RF algorithm can be employed for diverse studies containing data classification and image processing. An example of a hierarchical data structure is the decision tree. It resembles a real tree turned upside down. Each node in the decision tree, which has numerous nodes, is responsible for the test. Tree branches show potential elements of the chosen test, and they are left at the base of the tree to reflect the outcomes of the prediction. At the very top of the tree, the root node is defined [38].

3 Results and discussions

In this study, several scenarios are examined to understand how different influenced parameters impact classifications of the DGP. The parameters selected for the learning algorithm with their corresponding minimum and maximum values are listed in Table 1. Dataset samples that are applied in this survey are also shown in Table 2 (here, only three rows of data are illustrated). The influenced parameters as features are selected randomly between the throes range proposed in Table 1.

It is noteworthy to mention that DGP is selected as the target, which has four classifications. The other parameters in Table 2 are taken as features.

Before showing the validation of the different algorithm results, it is worth expressing that the evaluation index of DGP classifications techniques express how correctly they can predict the actual DGP classifications. In the literature, different error metrics are collected to quantify the precision of each sample founded on statistical error

Table 1: The range of the parameters utilized in the learning algorithms

The influenced parameter in the DGP	**Values**
luminance of the glare source (L_s)	1000 – 8000
source position index (P)	1.5 – 6.2
solid angle (ω)	0.01 – 0.31
vertical illuminance (lux)	100 – 20000

Table 2: The features and target parameters used in this study

lux	L_s	ω	**P**	**DGP**
2708	6343.8	0.09	2.3	Imperceptible
7855.7	3311	0.14	3.7	Intolerable
6988.3	1878.3	0.13	4	Disturbing
...	...	...	...	...

effects. However, in a classification task, the accuracy for a class shown in Equation (3.1) is expressed based on the True positive (TP), False positive (FP), True negative (TN), and False-negative (FN). The number of true positives (for instance) is the number of objects accurately marked as belonging to the positive class.

$$Accuracy = \frac{TP + TN}{TP + TN + FP + FN} \tag{3.1}$$

Table 3 listed the prediction accuracy of the DGP classifications by different algorithms.

Table 3: The machine learning algorithms' accuracy for DGP classification predictions

Machine learning techniques	**Accuracy (%)**
Random Forest	99
Support Vector Machine	98
Artificial Neural Network	97
K-Nearest Neighbors	88

Table 3 displays that all algorithms' accuracy is high, and our results are in good and excellent agreement with the actual data. Our results show that the RF has the highest accuracy compared with other techniques investigated in this study. By contrast, the KNN gives the lowest accuracy. Note that other methods, such as ANN and SVM, have high accuracy, which means that ANN, SVM, and RF represent very close and almost identical results.

ANN:

For constructing the layers of the ANN model, we employed four layers in which two layers with Relu activation are taken as hidden. Since we have considered the DGP has different classes (4 classes). Thus, the activation of the outer layer (fully contact layer) is selected as SoftMax. Figure 2 illustrates the model accuracy for the test and training. As can be seen after 50 epochs, the accuracy values remain almost constant (98%), which means that 50 epochs are enough for executing the ANN model. Moreover, for constructing the ANN model, we used TensorFlow, a free and open-source software library for machine learning and artificial intelligence. It can be utilized across various tasks but focuses on the training and inference of deep neural networks.

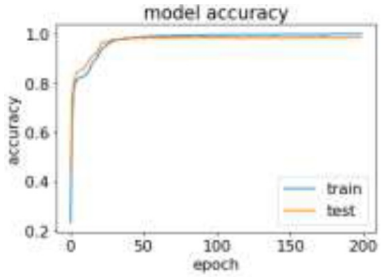

Figure 2: the model accuracy shows that the ANN model can predict the DGP classifications in high-value accuracy

SVM:

For the SVM selecting a proper kernel function play an important role in giving high-accuracy results. Our results showed that the linear kernel provides the highest accuracy, about 98%, and the sigmoid kernel gives the lowest accuracy, about 83%, respectively. We have examined two other kernel functions, Polynomial and Radial Basis Function (RBF), of which the accuracy was calculated at 87% and 95%, respectively.

KNN:

One of the simplest supervised machine learning methods is the idea behind the KNN algorithm. The KNN technique doesn't perform well with high-dimensional data because it has a lot of dimensions; it is hard for the algorithm to compute the distance in each dimension, despite being simple to implement. It calculates the separation between every training data point and a fresh data point. The K closest data points are then determined; K may be any integer. In the end, it assigns the data point to the class that includes the larger part of the K data points. In this study, we have chosen different values of the k to see which value is most effective, of which the k value equal to 10 has the highest accuracy.

RF:

Random Forest is a classifier that employs multiple decision trees on various subsets of the supplied dataset and adds the average to improve the dataset's predictive accuracy. One of the notable advantages of using classification and regression issues, which make up the majority of modern machine learning systems, is random forest. Some decision trees may predict the proper result, while others may not, since the random forest incorporates several trees to identify the class of the dataset. But when taken as a whole, all the trees make accurate predictions. Hence, downward are two hypotheses for a more suitable Random forest classifier:

- There should be some virtual values in the feature variable of the dataset so that the classifier can foresee objective results preferably than an assumed consequence.
- There must be extremely disgraceful connections in each tree's forecasts.

In this study, the RF algorithm illustrates the highest accuracy value, about 99.8%, among other considered methods. In addition to the DGP classification predictions, RF can also display the importance of the features on the results, as illustrated in Table 4. The RF results show that vertical illuminance (lux) strongly affects the DGP classification. By contrast, the influence of the other parameters on the DGP classifications is small.

Table 4: The significance of the features on the DGP classification predictions

Features	**Values (%)**
vertical illuminance (lux)	96.8
luminance of the glare source (Ls)	1.42
solid angle (ω)	0.98
source position index (P)	0.8

4 Conclusions

Since energy consumption, and hence CO_2 emission, is the current issue in society, the DGP is a critical element of the architectural design process. This study employed four well-known machine learning methods (ANN, KNN, SVM, and RF) to predict the DGP classifications. As this paper shows, machine learning is a powerful and promising technique to use in building construction. Based on multi techniques of machine learnings analysis, the following can be concluded:

- Random Forest gives the best prediction with an accuracy of 99.8%.
- Although the KNN results are agreeable, they provide the lowest accuracy at about 88%, among others.
- Vertical illuminance (lux) has the most effect on the DGP classification predictions.
- Under a wide range of investigated sunlight circumstances, Random Forrest is the most reliable measure and least likely to give misleading or erroneous glare forecasts, making it a useful tool for determining feature significance.

A vital advantage of the present study is that it is reasonably simple and applicable to other architectural design processes, such as Visual Comfort Probability (VCP). Furthermore, it is recommended to employ machine learning algorithms for the other glare metrics.

Index

NOMENCLATURE		Greek Symbols	
BR	v	A	source zone
Ls	The luminance of the glare source	I	distance between eyes and source
L_v	Vertical illuminance (lux)	θ	the angle from the source to the perpendicular plane on which a source is encountered
TP	True positive	$\omega = A\ \cos\theta/I^2$	Solid angle
FP	False positive	α	the angle between the line of sight, in degrees, (here, $\tan^{(-1)}(x/y)$) and the vertical of the plane including the source
TN	True negative	β	the angle between the line overlooking the source and the line of sight
FN	False negative	$P = \exp[(35.2 - 0.31889\alpha - 1.22e^{-2\alpha/9}) \times 10^{-3}\beta + (21 + 0.26667\alpha - 0.002936\alpha^2) \times 10^{-5}\beta^2]$	The source position index
		Subscripts	
		DGP	daylight glare probability
		ML	Machine Learning
		ANN	Artificial Neural Network
		KNN	K-Nearest Neighbors
		SVM	Support Vector Machines
		RF	Random Forest
		MLP	Multi-layer perceptron

References

[1] M.S. Barkhordari, M.S. Es-Haghi, *Straightforward prediction for responses of the concrete shear wall buildings subject to ground motions using machine learning algorithms*, Int. J. Eng. **34** (2021), no. 7, 1586–1601.

[2] J. Bromley and E. Sackinger, *Neural-network and k-nearest-neighbor classifiers*, AT&T Bell Laboratories, (1991), 11359–910819.

[3] R.D. Clear, *Discomfort glare: What do we actually know?*, Lighting Res. Techno. 45 (2013), 58–141.

[4] Commission Internationale de l'Eclairage CTC 3-13, *Discomfort glare in interior lighting*, Proc. CIE 21st Session, CIE Publication 117, Vienna: CIE, 1995.

[5] V. Derbentsev, V. Babenko, K. Khrustalev, H. Obruch and S. Khrustalova, *Comparative performance of machine learning ensemble algorithms for forecasting cryptocurrency prices*, Int. J. Eng. **34** (2021), no. 1, 140–148.

[6] H. Drucker, C.J. Burges, L. Kaufman, A. Smola, and V. Vapnik, *Support vector regression machines*, Adv. Neural Inf. Process. Syst. **9** (1997), 155–161.

[7] H.D. Einhorn, *Discomfort glare: A formula to bridge differences*, Lighting Res. Technol. 11 (1979), no. 2, 90–94.

[8] V.C. Handikherkar and V.M. Phalle, *Gear fault detection using machine learning techniques-a simulation-driven approach*, Int. J. Eng. **34** (2021), no. 1, 212–223.

[9] T. Hastie, R. Tibshirani, J.H. Friedman and J.H. Friedman, *The elements of statistical learning: Data mining, inference, and prediction*, Springer, New York, 2009.

[10] M.B. Hirning, *The application of luminance mapping to discomfort glare: A modified glare index for green buildings*, PhD diss., Queensland University of Technology, 2014.

[11] R.G. Hopkinson, *Glare from daylighting in buildings*, Appl. Ergon. **3** (1972), no. 4, 206–215.

[12] J.A. Jakubiec, *Validation of simplified visual discomfort calculations*, Build. Simul. Optim. Conf. (BSO2018), 2018, pp. 2–11.

[13] J.A. Jakubiec and C.F. Reinhart, *DIVA 2.0: Integrating daylight and thermal simulations using rhinoceros 3D, DAYSIM and EnergyPlus*, Proc. Build. Simul. 12th Conf. Int. Build. Perform Simul. Assoc. **20** (2011), no. 11, 2202–2209.

[14] J.A. Jakubiec and C. Reinhart, *The 'adaptive zone'–A concept for assessing discomfort glare throughout daylit spaces*, Lighting Res. Technol. 44 (2012), no. 2, 149–170.

[15] J.A. Jakubiec and C.F. Reinhart, *A concept for predicting occupants' long-term visual comfort within daylit spaces*, LEUKOS–J. Illum. Eng. Soc. North America, 12 (2016), no. 4, 185–202.

[16] M.G. Kent, S. Altomonte, P.R. Tregenza and R. Wilson, *Temporal variables and personal factors in glare sensation*, Light. Res. Technol. **48** (2016), 710–689.

[17] M. Khedmati, F. Seifi and M.J. Azizi, *Time series forecasting of Bitcoin price based on autoregressive integrated moving average and machine learning approaches*, Int. J. Eng. **33** (2020), no. 7, 1293–1303.

[18] I. Konstantzos, A. Tzempelikos and Y.C. Chan, *Experimental and simulation analysis of daylight glare probability in offices with dynamic window shades*, Build. Environ. **87** (2015), 244–254.

[19] T. Kruisselbrink, R. Dangol and A. Rosemann, *Photometric measurements of lighting quality: An overview*, Build. Environ. **138** (2018), 42–52.

[20] S. Kumar and G. Sahoo, *A random forest classifier based on genetic algorithm for cardiovascular diseases diagnosis (research note)*, Int. J. Eng. **30** (2017), no. 11, 1723–1729.

[21] D. Mah, M. Kim and A. Tzempelikos, *Utilization of programmable cameras for web-based sensing and control of daylight in buildings*, J. Phys.: Conf. Ser. **2042** (2021), no. 1, 012114.

[22] D.S. Maitra, U. Bhattacharya and S.K. Parui, *CNN based common approach to handwritten character recognition of multiple scripts*, 13th Int. Conf. Doc. Anal. Recog. (ICDAR), 2015, pp. 1021–1025.

[23] A. Mentens, S. Martin, F. Descamps, J. Lataire and V.A. Jacobs, *Daylight glare probability prediction for an office room*, Proc. CIE Midterm Meet., 2021.

[24] T.M. Mitchell, *Machine Learning*, McGraw-hill, New York, 2007.

[25] M. Namakshenas, *Real-time scheduling of a flexible manufacturing system using a two-phase machine learning algorithm*, Int. J. Eng. **26** (2013), no. 9, 1067–1076.

[26] A. Nazzal, Ö. Güler and S. Onaygil, *Subjective experience of discomfort glare in a daylit computerized office in Istanbul and its mathematical prediction with the DGIN method*, ARI Bull. Istanbul Tech. Univer. **54** (2005), no. 03, 96–107.

[27] B. Painter, D. Fan and J. Mardaljevic, *Evidence-based daylight research: Development of a new visual comfort monitoring method*, 11th Int. Light. Conf., Istanbul, Turkey, 2009.

[28] C. Pierson and M. Bodart, *Validation and universalization of daylight glare probability index*, LumeNet 2016, Ghent, Belgium, 2016, 82.

[29] C. Reinhart and A. Fitz, *Findings from a survey on the current use of daylight simulations in building design*, Energy Build. **38** (2006), no. 7, 824–835.

[30] F. Rosenblatt, *Principles of neurodynamics. perceptrons and the theory of brain mechanisms*, Cornell Aeronautical Lab Inc Buffalo NY, 1961.

[31] J.A.Veitch, *Light, lighting, and health: Issues for consideration*, LEUKOS–J. Illumin. Eng. Soc. North Amer. **2** (2005), no. 2, 85–96.

[32] M. Piechowski and A. Rowe, *Building design for hot and humid climates–implications on thermal comfort and energy efficiency*, IBPSA 2007–Int. Build. Perform. Simul. Assoc., 2007, pp. 122–126.

[33] G. Ward, *Rendering with radiance: The art and science of lighting visualization*, Morgan Kaufman, 1998.

[34] J. Wienold and J. Christoffersen, *Towards a new daylight glare rating*, Lux Europa, Berlin, 2005, pp. 157–161.

[35] J. Wienold and J. Christoffersen, *Evaluation methods and development of a new glare prediction model for daylight environments with the use of CCD cameras*, Energy Build. **38** (2006), no. 7, 743–757.

[36] J. Wienold and Fraunhofer Institute for Solar Energy Systems ISE, *Daylight glare in offices*, Fraunhofer Verlag, Alemanha, 2010.

[37] J. Wienold, T. Iwata, M. Sarey Khanie, E. Erell, E. Kaftan, R.G. Rodriguez, J.A. Yamin Garretón, T. Tzempelikos, I. Konstantzos, J. Christoffersen and T.E. Kuhn, *Cross-validation and robustness of daylight glare metrics*, Light. Res. Technol. **51** (2019), no. 7, 983–1013.

[38] J.A. Yamin Garretón, R.G. Rodriguez, A. Ruiz and A.E. Pattini, *Degree of eye opening: A new discomfort glare indicator*, Build. Environ. **88** (2015), 142–150.